

NASA CR 195248

19-20-010

UTK Research Account Number: R01-1372-59
Final Report

209781
22 p

"Verification of Thermal Analysis Codes for Modeling Solid Rocket Nozzles"

M. Keyhani
Associate Professor
Mechanical & Aerospace Engineering Department
The University of Tennessee
Knoxville, Tennessee 37996-2210

Submitted To:

Dr. Gerald R. Karr
Department of Mechanical Engineering
The University of Alabama in Huntsville
Huntsville, Alabama 35899

Sub Grant No. NASA/NAG8-212 Task 5

May, 1993

(NASA-CR-195248) VERIFICATION OF
THERMAL ANALYSIS CODES FOR MODELING
SOLID ROCKET NOZZLES Final Report
(Alabama Univ.) 22 p
N94-27150
Unclas
63/20 0209781

SUMMARY

One of the objectives of the Solid Propulsion Integrity Program (SPIP) at Marshall Space Flight Center (MSFC) is development of thermal analysis codes capable of accurately predicting the temperature field, pore pressure field and the surface recession experienced by decomposing polymers which are used as thermal barriers in solid rocket nozzles. The objective of this study is to provide means for verifications of thermal analysis codes developed for modeling of flow and heat transfer in solid rocket nozzles. In order to meet the stated objective, a test facility was designed and constructed for measurement of the transient temperature field in a sample composite subjected to a constant heat flux boundary condition. The heating was provided via a steel thin-foil with a thickness of 0.025 mm. The designed electrical circuit can provide a heating rate of 1800 W. The heater was sandwiched between two identical samples, and thus ensure equal power distribution between them. The samples were fitted with Type K thermocouples, and the exact location of the thermocouples were determined via X-rays. The experiments were modeled via a one-dimensional code (UT1D) as a conduction and phase change heat transfer process. Since the pyrolysis gas flow was in the direction normal to the heat flow, the numerical model could not account for the convection cooling effect of the pyrolysis gas flow. Therefore, the predicted values in the decomposition zone are considered to be an upper estimate of the temperature. From the analysis of the experimental and the numerical results the following are concluded.

- i) The virgin and char specific heat data for FM 5055 as reported by SoRI (values and references given in Appendix A) can not be used to obtain any reasonable agreement between the measured temperatures and the predictions. However, use of virgin and char specific heat data given in Acurex report [1] produced good agreement for most of the measured temperatures.
- ii) Constant heat flux heating process can produce a much higher heating rate than the radiative heating process. The results show that heating rates of 125 °C/s (225 °F/s) can be achieved.
- iii) The electrical resistance of the FM 5055 samples were about 150 Ω in the virgin state, and decreased to about 35 Ω when charred. A reliable scheme must be developed to electrically insulate the composite from the heater foil in order to prevent any current leakage into the sample which can result in volumetric heating of the char zone of the composite.

ACKNOWLEDGMENT

This sub grant from The University of Alabama, Huntsville is funded by NASA Marshall Space Flight Center (MSFC). The grant monitors at The University of Alabama and the MSFC are, respectively, Drs. Gerald Karr and Ken McCoy. Their guidance is greatly appreciated.

I also would like to acknowledge the help and support of other MSFC personnel, among them, Mr. Jim Owen, Mr. Louie Clayton, Dr. Roy Sullivan, and Mr. Glenn Jamison.

TABLE OF CONTENTS

	<u>Page</u>
SUMMARY	ii
ACKNOWLEDGMENT	iii
NOMENCLATURE	v
I. EXPERIMENTAL APPARATUS AND PROCEDURE	1
I.1 Overview	1
I.2 Experimental Apparatus	1
I.3 Experimental Procedure	4
II. RESULTS AND DISCUSSION	5
II.1 Numerical Model	5
II.2 Experimental Results	6
III. CONCLUSIONS	12
REFERENCES	13
APPENDICES	
A. FM 5055 PROPERTIES	14

NOMENCLATURE

C_p	Specific heat
F	View factor
h	Convection heat transfer coefficient
H	Sample thickness in the direction of heat flow (y direction)
k	Thermal conductivity
q''	Input surface heat flux
t	Time
t_f	Final heating time
T	Temperature
T_i	Initial Temperature
T_∞	Ambient temperature for convection cooling
T_s	Surface temperature of the heated sample
T_{sur}	Surrounding temperature for radiation heat loss
W	Sample width in the direction normal to heat flow (x direction)
x	Coordinate system normal to the direction of heat flow
y	Coordinate system in the direction of heat flow, measured from the heater surface

Symbols

β	Degree of Char
δ	Cement thickness
ϵ	Surface emissivity of the sample
ρ	Density

Subscripts

v	Virgin
c	Char

I. EXPERIMENTAL APPARATUS AND PROCEDURE

I.1 Overview

One of the objectives of the Solid Propulsion Integrity Program (SPIP) at Marshall Space Flight Center (MSFC) is development of thermal analysis codes capable of accurately predicting the temperature field, pore pressure field and the surface recession experienced by decomposing polymers which are used as thermal barriers in solid rocket nozzles. The objective of this study is to provide means for verifications of thermal analysis codes developed for modeling of flow and heat transfer in solid rocket nozzles. In order to meet the stated objective, a test facility was designed and constructed for measurement of the transient temperature field in a sample composite subjected to a constant heat flux boundary condition. The description of the experimental apparatus and procedure follows.

I.2 Experimental Apparatus

The components of the experimental setup are outlined in Figure 1. A Sorensen AC Regulator, model ACR 3000, was used to supply power to a transformer rated for 20 amps and 115 VAC. A Hewlett Packard 6634A DC power supply was used to activate the 15 amp Electrolet Killart relay to close the circuit to a Square D Company 2 KVA dry type single phase transformer which provided low voltage, high current power to the heating element. A 250 amp current shunt was placed in series with the circuit for current measurements.

Test Enclosure. Details of the test enclosure are shown in Figure 2. A steel cover with a 0.63 cm thick plexiglas front window was placed over the test area. Copper bars, measuring 0.63 cm x 1.27 cm x 20.32 cm, were used to provide the voltage input to the foil heater. To create the heated surface stainless steel foil, 0.025 mm thick, was clamped between the copper bars by tightening screws in the bars. Two tubes with funnels on the ends were connected to a helium tank to cool the edges of the heater next to the copper bars to prevent melting of the foil.

Test Samples. FM 5055 carbon-phenolic samples 1 cm x 2 cm x 4 cm were used as test specimen. The ply orientation and location of the thermocouples are shown in Figure 3. Two samples were clamped onto the upper and lower sides of the steel foil using C clamps as shown in Figure 2. In order to electrically insulate the samples from the heater foil a thin layer of No. 10 Sauereisen high temperature cement was applied to upper and lower surface of the steel heater foil. At room temperature thermal conductivity of this cement is approximately 74% higher than the virgin sample, and its specific heat is approximately the same as Virgin sample as reported by SoRI (see Appendix A). This cement can stand temperatures up to 1600 °C. The details of the sample-heater assembly are shown in Figure 4. The upper sample was instrumented with five AWG-36 (0.127 mm) type K thermocouples. The thermocouple beads were located at various y locations (measured from the heater surface) at z = 2 cm plane along the x = 1.0 cm line as shown in Figure 3. In order to minimize the disturbance to the sample material two of the thermocouples were inserted from the x = 0 surface and the others from the x = 2 cm surface. The thermocouples were inserted in drilled holes which were 1 cm long with a diameter of 0.76 mm. The void between the thermocouples and the sample material in the holes were filled by the high thermal conductivity cement.

Data Acquisition System. A Hewlett Packard 9000 Series 217 computer was used to control the power supply and the data acquisition system. The Hewlett Packard 3456A Digital Voltmeter with the Hewlett Packard 3497A Data Acquisition/Control Unit was used to record the voltage drop, the voltage across the current shunt, and voltage readings from the five type K thermocouples. A Kaye Ice Point Reference was used as the reference voltage for calculation of the temperatures of the thermocouples. Voltage drop across the steel foil was also measured using a Metex M-3610 voltmeter. Voltage across the current shunt was also measured using a Kiethley 177 Microvolt DMM with a Gould Brush 2400 chart recorder to obtain current as a function of time.

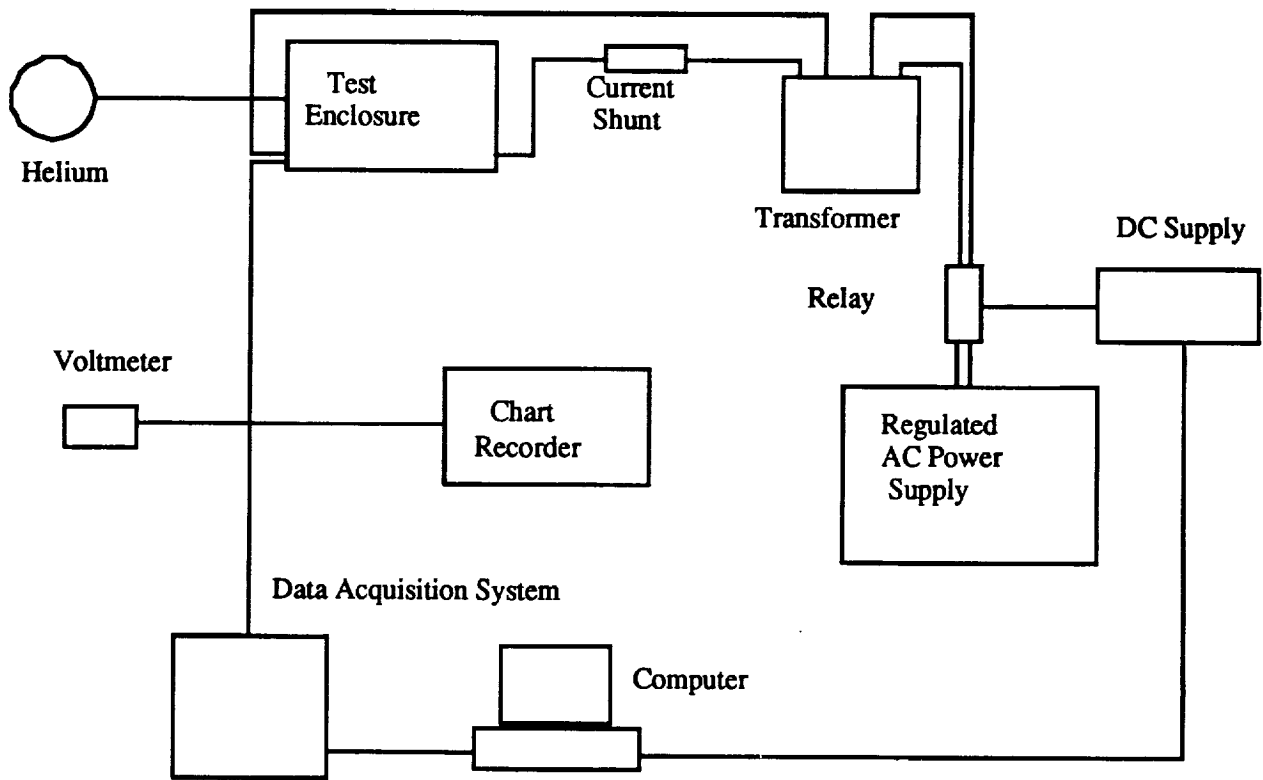


Figure 1. Schematic of the experimental setup

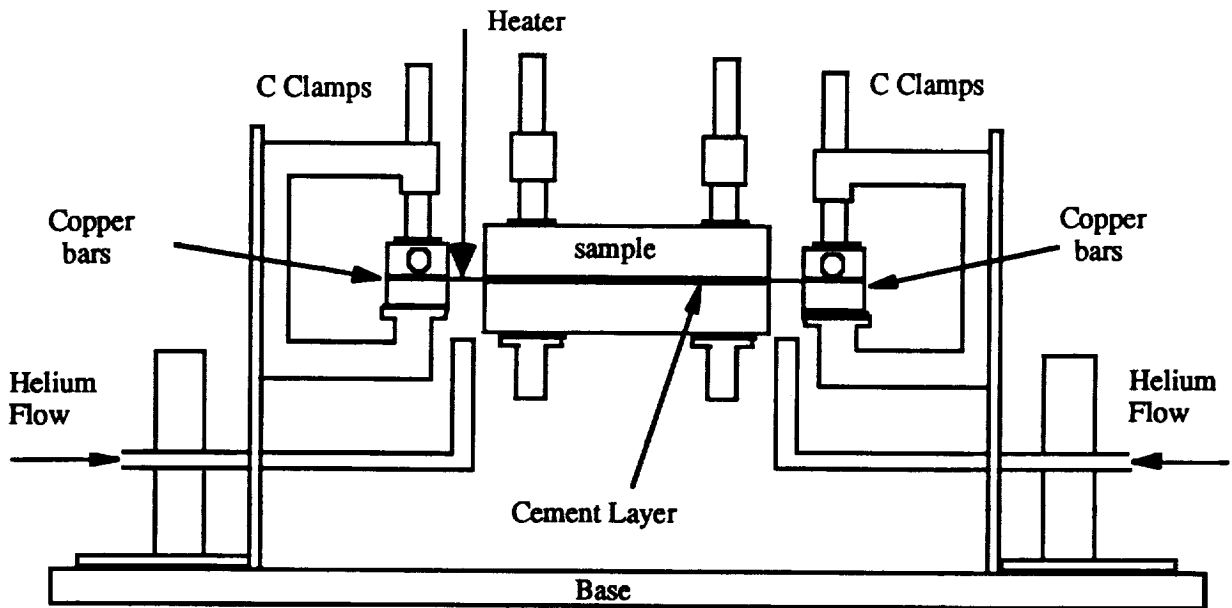


Figure 2. Details of the test enclosure

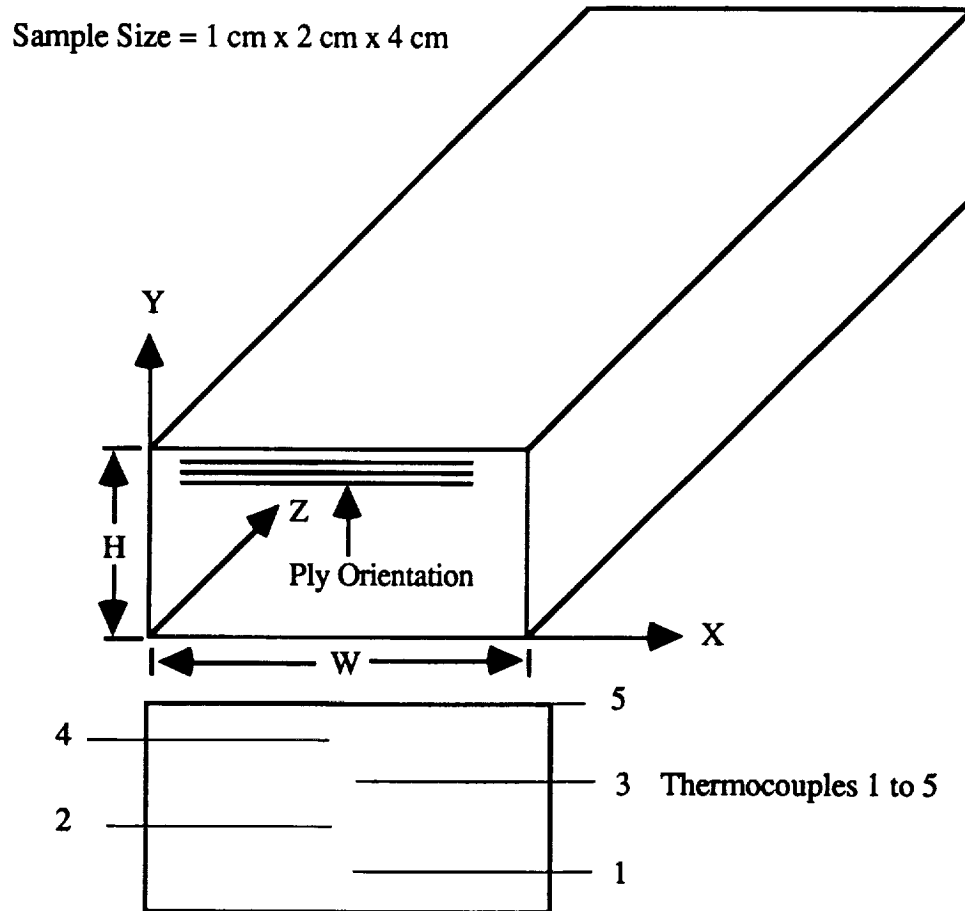


Figure 3. Description of the test sample

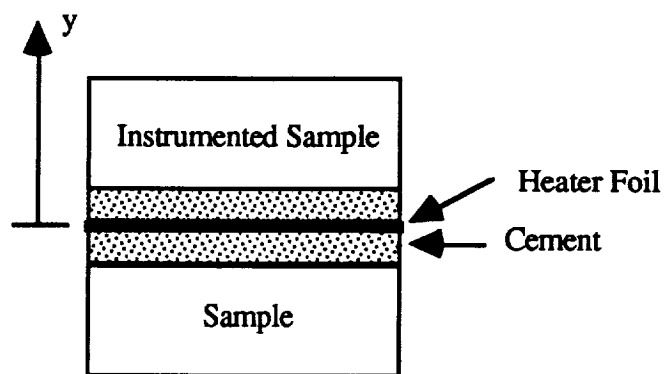


Figure 4. Details of the test sample-heater assembly

I.3 Experimental Procedure

Preparation. The Instrumented samples were X-rayed and the accurate location of the thermocouple beads were determined from the X-rays. Four samples were tested and the location of the thermocouples for these samples are given in Table 1. It should be noted that the x-location values listed in Table 1 merely represent the distance of the thermocouple bead to the x face, $x=0$ or $x=W$, from which the thermocouple was inserted. Initial mass of the uninstrumented samples were recorded, and a thin layer of No. 10 Sauereisen high temperature cement was placed on both sides of the stainless steel foil to prevent any leakage of electric current into the samples. Thin sheets of mica were placed along the sides of the samples and the copper bars.

Table 1. Thermocouple locations for the tested samples

Sample No. width (mm) height (mm)	Thermocouple Number	X Location (mm)	Y Location (mm)
1 W = 20.12 H = 9.98	1	8.130	2.840
	2	10.31	4.320
	3	5.870	6.530
	4	10.31	8.280
	5	10.16	10.64
2 W = 20.27 H = 10.03	1	8.130	4.440
	2	10.52	5.730
	3	6.020	7.870
	4	10.47	9.620
	5	10.36	12.03
3 W = 20.22 H = 9.98	1	9.930	1.936
	2	10.87	4.346
	3	9.400	5.796
	4	9.650	7.696
	5	10.80	10.01
4 W = 20.32 H = 10.06	1	10.85	2.720
	2	9.320	4.960
	3	8.740	5.880
	4	8.530	8.320
	5	9.530	10.52

Operation. The ice point reference unit was running continuously before the experiment to assure an accurate reading of the reference thermocouple. The Hewlett Packard Digital Voltmeter and all the other recording devices were turned on, and the zero offsets of the meters were recorded. The video camera was run to record the date and then left on to record with the stopwatch display. The power supply voltage was set, and the program was started on the HP computer. A stopwatch was operated by hand to record heating time in the event that the steel foil melted before the programmed time duration was reached. The helium flow was started. The computer closed the relay, and the heat flux was supplied to the sample at the determined power level and for the desired time. The pyrolysis gases released were videotaped for all runs. Voltage, current, and thermocouple temperatures were recorded. Final mass of the uninstrumented sample was recorded.

Data Reduction. The thermocouple voltages were recorded by the Hewlett Packard Digital Voltmeter, and the HP computer program converted them to temperatures, °C, by subtracting the ice point reference voltage and using an 8th order polynomial. Voltage drop across the steel foil was recorded by the HP computer program at the start and end of the run. Current was also

recorded by the HP computer at the start and end of the run. Current in amps was obtained by dividing the recorded voltage by the resistance of the current shunt. Time was measured by the HP computer at the start of the power, at the start of the thermocouple readings, and at the conclusion of the run when power was turned off. A time for each thermocouple reading was assigned by the HP computer. After the run was completed, the number of thermocouple readings, times, and thermocouple temperatures were written to an ASCII data file. Further details on experimental apparatus and procedure are given in [4].

II. RESULTS AND DISCUSSION

II.1 Numerical Model

A one-dimensional numerical code (UT1D) developed by Krishnan and Keyhani [2,3] was used to predict the experimental results. The experimental conditions, namely the sample size, heating condition, and the location of the thermocouples are a good representation of a one-dimensional transient conduction with phase change heat transfer phenomenon. Since the plies in the samples were normal to the direction of the heat flow (plies are parallel to the x direction), and the permeability in the with ply direction is much higher than the across ply direction, most of the pyrolysis gas flow in the experiments were in the x direction. Therefore, the convection cooling effect of the pyrolysis gases can not be modeled with a one-dimensional code. Thus, the code should over predict the temperatures in the decomposition zone. The input heat flux, initial temperature and the dimensions of the samples for the four experiments are given in Table 2. The boundary conditions in the numerical model are as follows:

$y = 0$: constant heat flux input q'' equal the experimental value

$y = H + \delta$: convection cooling with $h = 4.9 \times 10^{-4}$ BTU/ft²·s·R, $T_{\infty} = \text{experimental } T_i$
radiation heat loss to surroundings with $T_{\text{sur}} = T_i$, $\epsilon = 0.9$, $F = 1.0$

For the experimental temperature range of the back surface, a heat transfer coefficient of 4.9×10^{-4} BTU/ft²·s·R is a typical value for natural convection from a heated surface facing upward. In experiments with samples 1, 2 and 4 the heater foil was covered with a layer of cement with specified thickness as shown in Table 2. This cement layer was modeled in each case with the following cement properties:

$$\rho = 146 \text{ lbm/ft}^3; \quad C_p = 0.235 \text{ BTU/lbm}\cdot\text{R}; \quad k = 4.6 \times 10^{-4} \text{ BTU/ft}\cdot\text{s}\cdot\text{R}$$

In experiment with sample 3 a very thin layer of mica (0.03 mm) was used to electrically insulate the sample which was neglected in the numerical model. The FM 5055 properties used in the numerical model are given in Appendix A.

Table 2. Input heat flux, initial temperature and heating time for the tested samples

Sample No.	Initial Temp. (°C)	Heat Flux (W/cm ²)	Heating Time (sec)	Cement Thickness δ (mm)	Initial Mass (gm)	Final Mass (gm)	% Mass Loss
1	25.6	30.5	28.6	0.66	11.8230	11.3727	3.81
2	26.8	33.0	23.2	2.0	11.8240	11.4315	3.32
3	27.3	36.5	24.4	NONE*	11.8238	11.2150	5.15
4	21.5	30.6	28.1	0.46	11.8219	11.3998	3.57

* electrical insulation was provided via a 0.03 mm layer of mica

II.2 Experimental Results

Sample 4. The best agreement with the experimental results were obtained for this sample, and it will be presented first. The FM 5055 properties listed Appendix A were compiled from SoRI reports and Acurex report (ref. 1). For the specific heat of the sample data are available from both sources. The predicted temperatures using SoRI specific heat values for FM 5055 and the measured temperatures are presented in Figure 5.

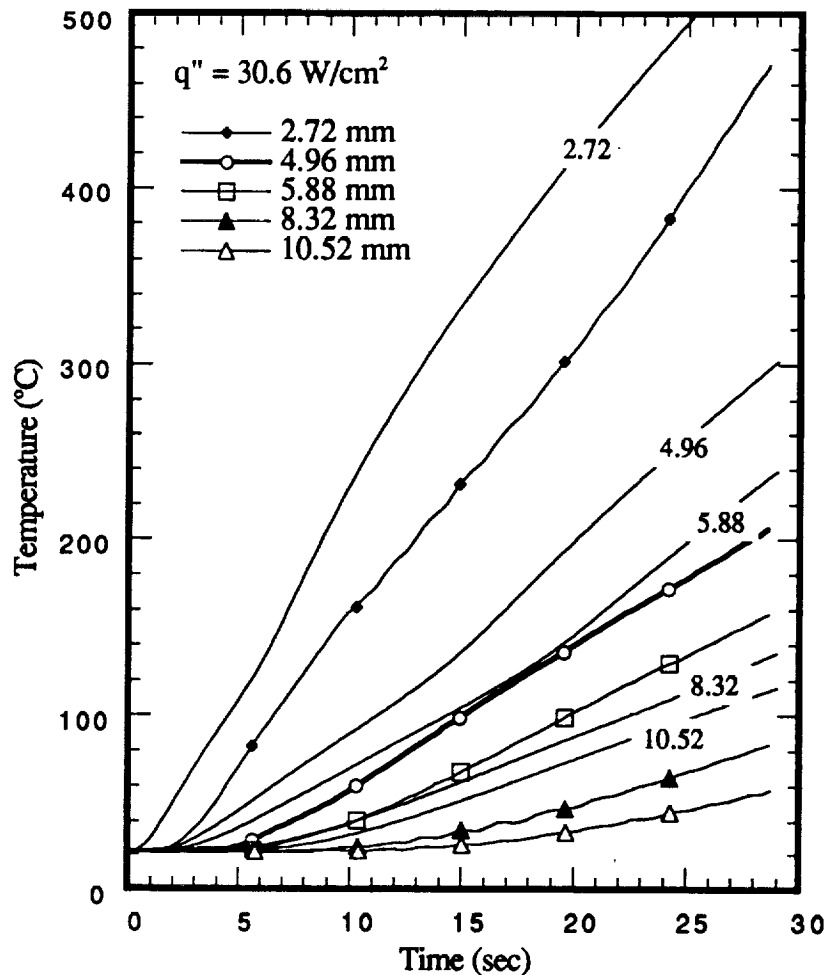


Figure 5. Comparison of sample 4 data with the numerical predictions using SoRI C_p data

It can be seen clearly that the predicted values at all five locations are substantially higher than the measured values. For example at $y = 5.88 \text{ mm}$, $t = 28 \text{ s}$ the experimental value is $154 \text{ }^\circ\text{C}$ while the predicted temperature is $224 \text{ }^\circ\text{C}$. Since decomposition of FM 5055 does not begin at temperatures below $286 \text{ }^\circ\text{C}$ (1009 R) it can be stated that except thermocouple 1 located at $y = 2.72 \text{ mm}$, the other locations are only experiencing conduction heat transfer without any phase change. As noted earlier, the convection cooling effect of the pyrolysis gases is not modeled in the numerical prediction shown. However, numerical experiments with convection cooling modeled as flowing towards the heated surface reduced the predicted temperature at $y = 2.72 \text{ mm}$ location by $30 \text{ }^\circ\text{C}$ at $t = 30 \text{ s}$, and had no appreciable effect on the predicted values for other y locations. In

summary, the specific heat values reported by SoRI were suspected to be too low. Therefore, the rest of predictions are based on virgin and char C_p values given by Ross and Strobel in an Acurex report [1]. For the experimental temperature range encountered the Acurex report C_p values for the virgin and char components are constant at 0.41 BTU/lbm·R. The predicted temperatures using Acurex report [1] specific heat values for FM 5055 and the measured temperatures are presented in Figure 6.

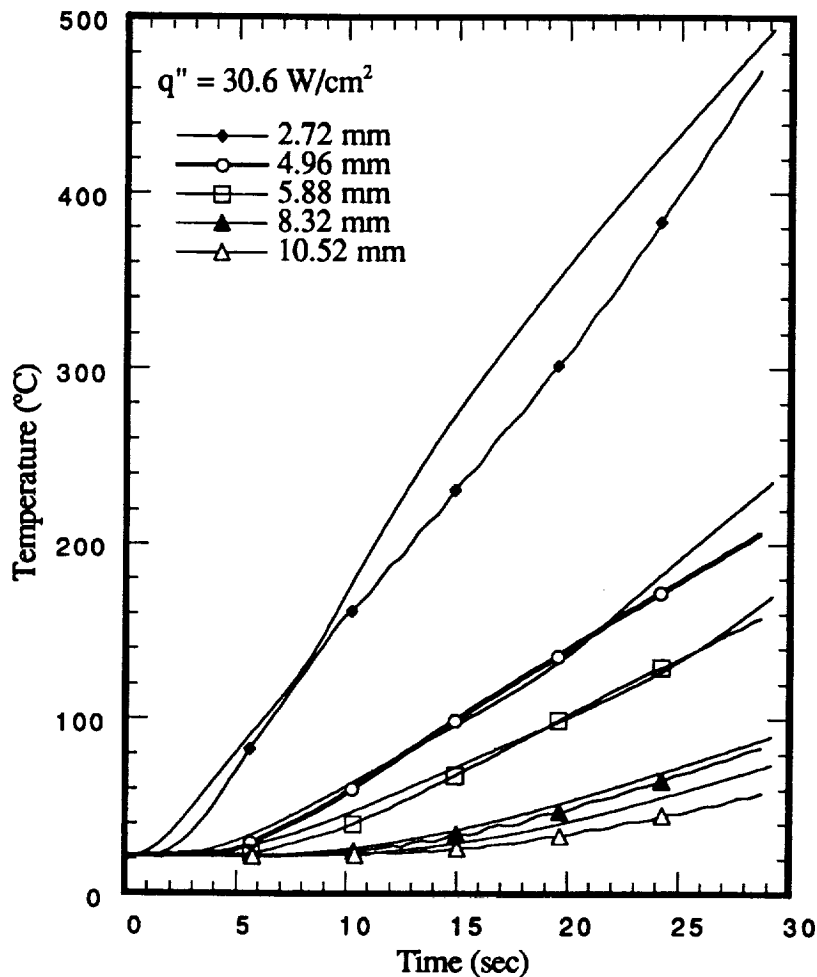


Figure 6. Comparison of sample 4 data with the numerical predictions using Ref. [1] C_p data

Figure 6 shows that the numerical predictions are in a very good agreement with the measured in-depth values at locations $y = 4.96, 5.88$ and 8.32 mm. The temperature range for these locations are in the conduction heat transfer regime. However, at $y = 2.72$ mm where the measured temperature is in the decomposition range, the numerical predictions are higher than the measured values. It was noted that the code should predict higher values in the decomposition zone since the convection cooling effect is not modeled. One should note that for correct modeling of the convection cooling effect a two-dimensional code should be used since almost all of the gas flow is in the direction normal to the heat flow. A wavy behavior at $y = 8.32$ and 10.52 mm experimental data is observed which is believed to be due to slight AC current leakage through the cement into

the sample. In order to render a judgment on the comparison of the data with the predictions one should consider the uncertainties in the thermophysical properties, sample variations, thermocouple locations, measured power and temperatures, and finally the limitations of the model. In view of these uncertainties and limitations, the observed comparison in Figure 6 is indeed encouraging.

Sample 1. In this experiment the heater foil was covered with a 0.66 mm layer of cement (0.2 mm more than sample 4), the power input was 30.5 W/cm² (0.33% less than sample 4 case), and the initial temperature was 25.6 °C (4.2 °C more than sample 4 case). The comparison of the predicted values for this sample with the experimental results are shown in Figure 7.

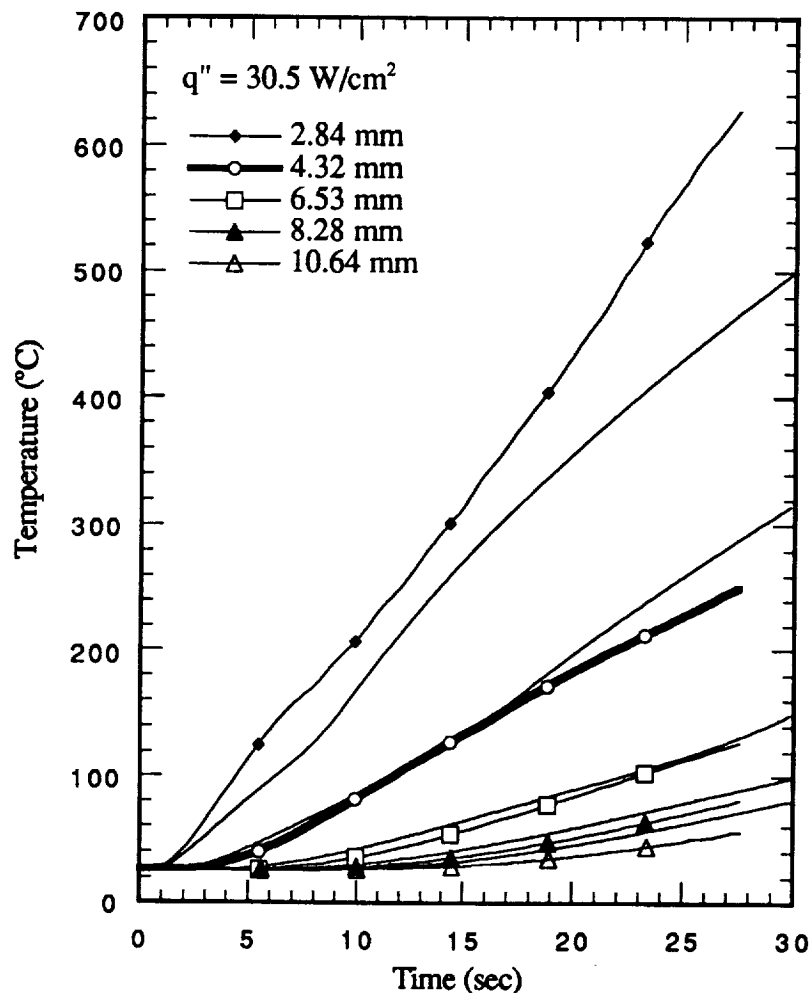


Figure 7. Comparison of sample 1 data with the numerical predictions using Ref. [1] C_p data

For this sample one would expect that for the same location the measured temperatures, after accounting for 4.2 °C higher initial temperature, should be close to those of sample 4. For thermocouple 4 and 5 this indeed is the case. However, thermocouple 1 located at $y = 2.84$ mm (0.12 mm farther from the heater than thermocouple 1 in the sample 4) is indicating a much higher temperature than that of sample 4 case. This is clearly unexpected. The X-ray for this sample was re-examined, and the following explanation can be offered. A guide was used to ensure that the holes drilled in the samples were 10 mm long. Table 1 shows that x-location of the thermocouple 1

in sample 1 was measured to be 8.13 mm. This indicates that about the last 2 mm of this hole was an air void which does not show in the X-ray. Therefore, this thermocouple was not covered with cement, and thus was not electrically insulated. The virgin FM 5055 samples had a resistance of about 150 Ω , and their resistance after heating was reduced to about 35 Ω . Moreover, the cement's resistance to electrical flow reduces by a factor of 100 when it is heated from room temperature to about 800 $^{\circ}\text{C}$. Since the filter on HP voltmeter was turned off for faster data collections, it is possible that this thermocouple readings were affected by the AC voltage drop in the sample.

Sample 2. In this experiment the heater foil was covered with a 2 mm layer of cement, which placed the first thermocouple at 4.44 mm from the heated surface. The results show that the measured locations were experiencing a conduction heat transfer phenomenon. The comparison of the predicted values for this sample with the experimental results are shown in Figure 8.

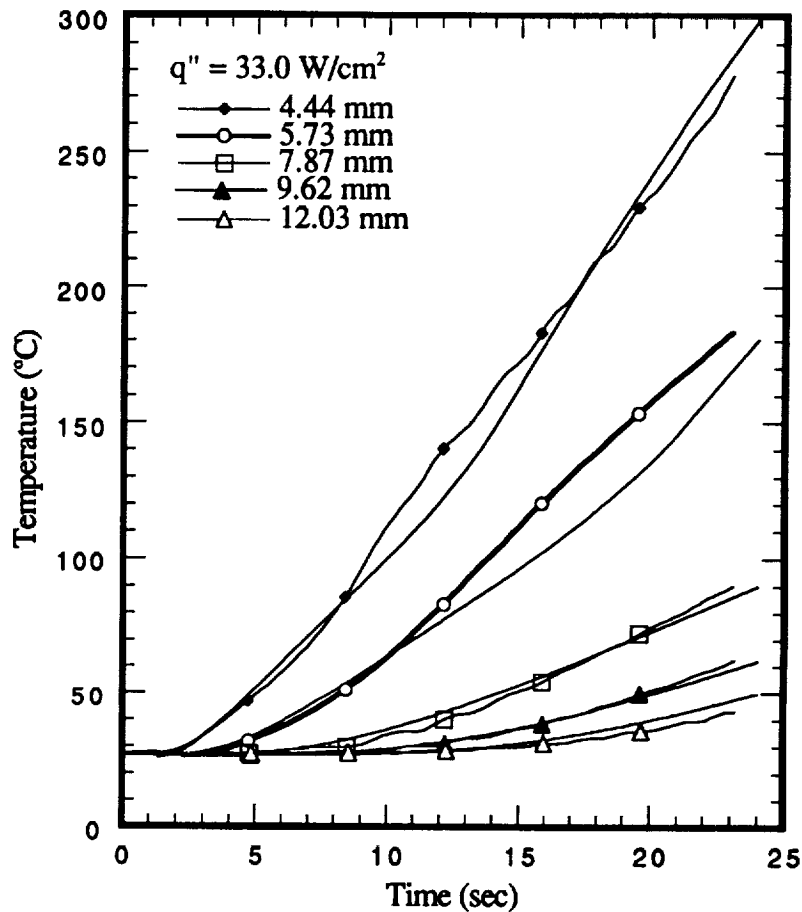


Figure 8. Comparison of sample 2 data with the numerical predictions using Ref. [1] C_p data

In order to have the proper perspective for analysis of the results and predictions for this case, the degree of char and the temperature profiles at $t = 24$ s are shown in Figure 9. It can be observed that the degree of char is less than 1% for the regions with $T < 300$ $^{\circ}\text{C}$. Moreover, the degree of the char varies from 65% at the sample surface ($y = 2$ mm) to 10% at $y = 3$ mm. That is the first 1 mm of the FM 5055 has experienced substantial decomposition. The fact that the data of this sample, measured in the conduction heat transfer zone of the sample, can be predicted with reasonable accuracy suggests that the decomposition zone heat transfer ($y = 2$ to 3 mm) has been properly modeled. Furthermore, it suggests that the thermophysical properties are certainly adequate for the conduction heat transfer regime.

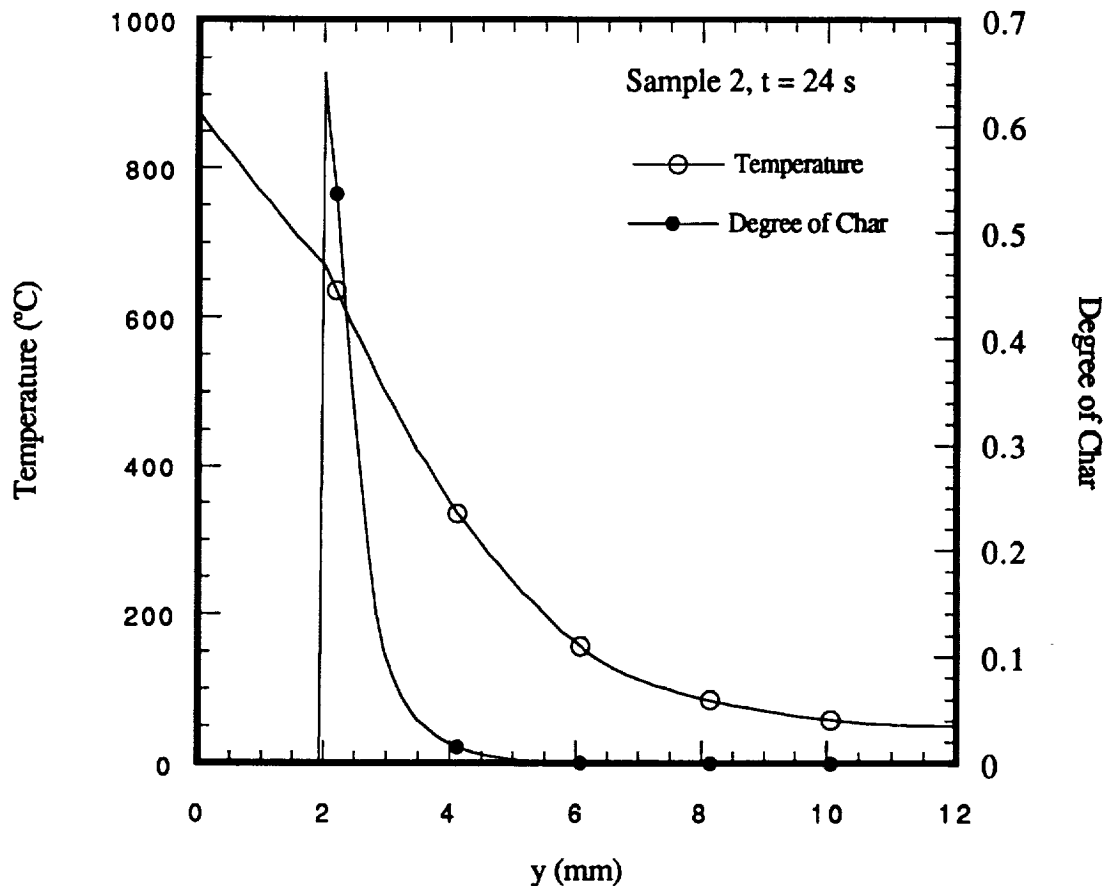


Figure 9. Predicted degree of char and temperature profiles for sample 2 at $t=24$ s (Ref. [1] C_p data)

Sample 3. A 0.03 mm of mica was used to electrically insulate the sample from the foil heater. The measured temperatures for this test are presented in Figure 10 along with the numerical predictions. The agreements between the predicted values and measured temperatures for locations $y = 4.35$ mm, 5.8 mm, 7.7 mm and the back face ($y = 10.01$ mm) are fairly good and encouraging. It may be noted that the predicted back face temperatures (exposed to the laboratory environment) for all the samples are higher than the measured temperatures. This may be partially due to a low convection heat transfer coefficient used for modeling the heat loss. Another cause may be the heat sink effect of the C clamps (in contact with the back face) used to keep the sandwich sample-heater-sample assembly together. The predicted temperature for thermocouple 1 ($y = 1.94$ mm) is in good agreement up to 12 s into the transient were the temperature reaches a value of about 320 °C. For $t > 12$ s the measured values start departing from the predicted temperature and the difference increases with time. Mica losses its electrical resistance as it is heated, and in the temperature range of 700 to 900 °C crystallizes and ceases to be an electrical insulation. It is interesting to note that at $t = 12$ s (when the predictions and data start to differ) the predicted surface temperature is 770 °C which is just in the range for current leakage into the sample begin. Current leakage into the sample can cause volumetric induction heating close to the surface where the sample electrical resistance has been reduced due to charring. This may be another plausible and even better explanation for rapid and substantial rise in the measured temperature of thermocouple 1 in the sample 1 test. It may be noted

that in that case the measured value was higher than the prediction from the start of the transient, and the difference increased with time.

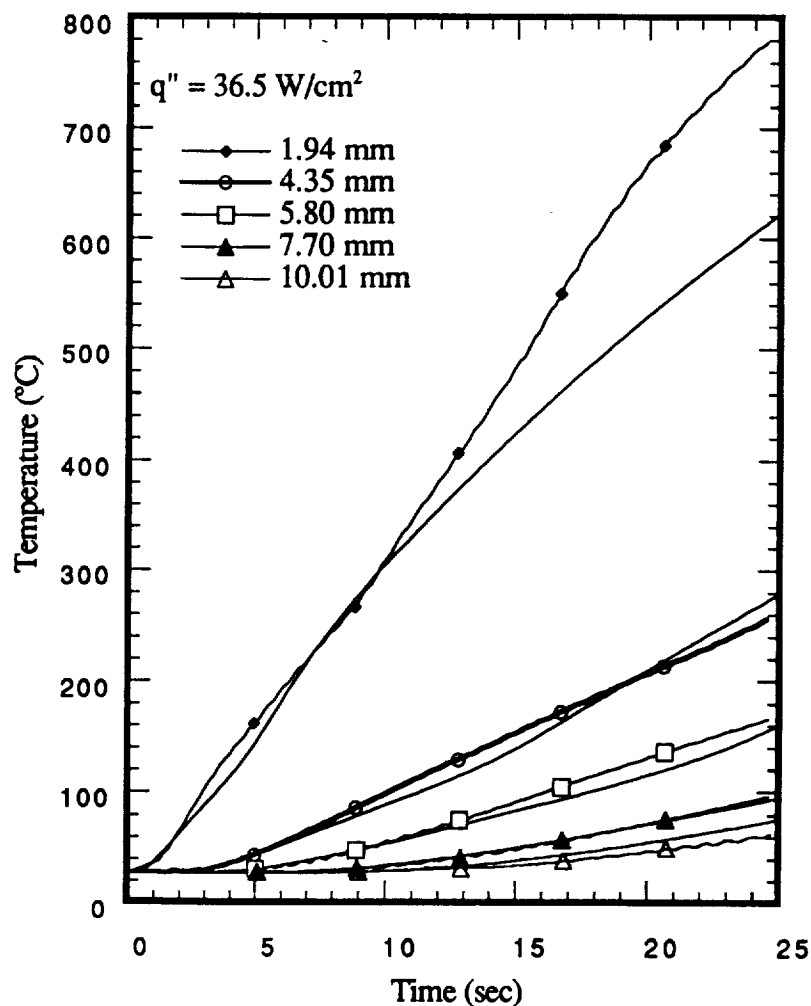


Figure 10. Comparison of sample 3 data with the numerical predictions using Ref. [1] C_p data

Heating Rate. The measured temperatures in the four tests show the heating rate at the measured locations. For sample 3 test the temperature at $y = 1.94 \text{ mm}$ shows an average heating rate of $28.4 \text{ }^\circ\text{C/s}$ ($51 \text{ }^\circ\text{F/s}$) in the time interval of $t = 0$ to 10 s . Clearly the locations closer to the surface were experiencing a higher heating rate. In order to get an estimate of the highest heating rate, the predicted FM 5055 surface temperatures are presented in Figure 11. The highest heating rate occurred in the sample 3 case which had the highest heat flux input and a 0.03 mm layer of mica for electrical insulation. Figure 11 shows that the average surface heating rate for sample 3 in the time interval of $t = 0$ to 4 s is about $125 \text{ }^\circ\text{C/s}$ ($225 \text{ }^\circ\text{F/s}$). Clearly constant heat flux heating process can produce a much higher heating rate than the radiative heating process.

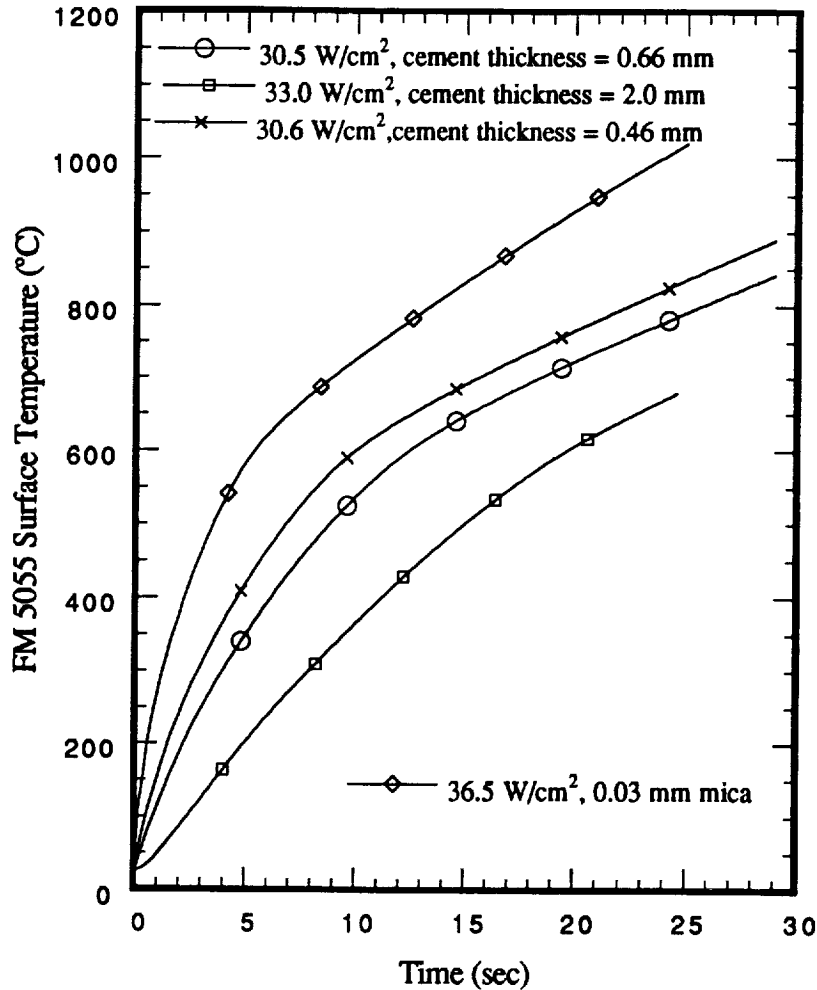


Figure 11. The predicted sample surface temperature history using Ref. [1] C_p data

III. CONCLUSIONS

An experimental facility for constant heat flux heating of carbon phenolic composite samples has been designed, fabricated and tested. The experiments were modeled via a one-dimensional code (UT1D) as a conduction and phase change heat transfer process. Since the pyrolysis gas flow was in the direction normal to the heat flow, the numerical model could not account for the convection cooling effect of the pyrolysis gas flow. Therefore, the predicted values in the decomposition zone are considered to be an upper estimate of the temperature. From the analysis of the experimental and the numerical results the following are concluded.

- i) The virgin and char specific heat data for FM 5055 as reported by SoRI (values and references given in Appendix A) can not be used to obtain any reasonable agreement between the measured temperatures and the predictions. However, use of virgin and char specific heat data given in Acurex report [1] produced good agreement for most of the measured temperatures.

- ii) Constant heat flux heating process can produce a much higher heating rate than the radiative heating process. The results show that heating rates of 125 °C/s (225 °F/s) can be achieved.
- iii) The electrical resistance of the FM 5055 samples were about 150 Ω in the virgin state, and decreased to about 35 Ω when charred. A reliable scheme must be developed to electrically insulate the composite from the heater foil in order to prevent any current leakage into the sample which can result in volumetric heating of the char zone of the composite.

REFERENCES

1. Ross, R., and Strobel, F., "CMA90S Input Guide and User's Manual," Acurex Corporation, December, 1990.
2. Krishnan, V., and Keyhani, M., " A One-Dimensional Thermal Model With an Efficient Scheme for Surface Recession," Proceedings of the 1992 JANNAF Rocket Nozzle Technology Subcommittee Meeting, Lockheed Missiles and Space Company, Sunnyvale, CA.
3. Krishnan, V., " A One Dimensional Model for the Thermal Response of a Decomposing Polymer, " M.S. Thesis, University of Tennessee, Knoxville, TN, 1992.
4. Pitman, F., "An Experimental Study of Thermal Response of Decomposing polymers," M.S. Thesis, University of Tennessee, Knoxville, TN., in progress.

APPENDIX A

FM 5055 PROPERTIES

FM 5055 PROPERTIES

Source 1: CMA90S Input Guide and User's Manual," Acurex Corporation, December, 1990.
 Source 2: Southern Research Institute, SRI-MME-91-056-6672-003
 Source 3: Southern Research Institute, SRI-EAS-88-201-6032-1
 Source 4: Stokes, E. H., Compressibility of Carbon-Phenolic Pyrolysis Gas Products and a Discussion of Other Factors Contributing to Internal Gas Pressure Calculations.

DECOMPOSITION KINETIC DATA, From Source 1, Sample 2

React	ρ_v lb/ft ³	ρ_c lb/ft ³	Pre-Exp fact. 1/sec	React. order	E/R R	T-react R
A	15.48	0.0	0.2171E2	1.92	0.8329E4	536
B	0.0	0.0	0.1000E1	1.00	0.1000E1	9900
C	139.28	118.98	0.9535E11	3.10	0.3480E5	1009

VIRGIN HEAT OF FORMATION, From Source 1, Sample 2
 -391.72 BTU/lbm

CHAR HEAT OF FORMATION, From Source 1, Sample 2
 0.0 BTU/lbm

RESIN FRACTION, From Source 1, Sample 2
 0.401

VIRGIN WITH PLY THERMAL CONDUCTIVITY, From Source 3, Fig 3.2-2

T, R	k, BTU/ft-s-R
610.0	0.000181
760.0	0.000238
860.0	0.000248
960.0	0.000248
1060.0	0.000245
1160.0	0.000241

VIRGIN ACROSS PLY THERM. CONDUCTIVITY, From Source 3, Fig 3.2-1

T, R	k, BTU/ft-s-R
610.0	0.000130
760.0	0.000148
860.0	0.000157
960.0	0.000164
1060.0	0.000167
1160.0	0.000162

CHAR WITH PLY THERMAL CONDUCTIVITY, From Source 3, Fig 3.2-5

T, R	k, BTU/ft-s-R
660.0	0.000257
860.0	0.000299
1060.0	0.000324
1260.0	0.000354
1460.0	0.000377
1660.0	0.000403
1960.0	0.000440

CHAR ACROSS PLY THERM. CONDUCTIVITY, From Source 3, Fig 3.2-4

T, R	k, BTU/ft-s-R
660.0	0.000153
860.0	0.000188
1060.0	0.000218
1260.0	0.000243
1460.0	0.000264
1660.0	0.000269
1960.0	0.000269

VIRGIN HEAT CAPACITY, From Source 3, Fig 3.3-2

T, R	c, BTU/lbm-R
560.0	0.230
660.0	0.285
760.0	0.310
860.0	0.328
960.0	0.345
1060.0	0.355

CHAR HEAT CAPACITY, From Source 3, Fig 3.3-4

T, R	c, BTU/lbm-R
560.0	0.205
660.0	0.240
760.0	0.272
860.0	0.295
960.0	0.320
1060.0	0.345
1160.0	0.360
1260.0	0.375
1360.0	0.388
1460.0	0.400
1560.0	0.410
1660.0	0.420
1760.0	0.424
1860.0	0.429
1960.0	0.432

PYROLYSIS GAS ENTHALPY, From Source 1, Sample 2

T, R	h, BTU/lbm
530.0	-1574.2
1000.0	-1175.4
1500.0	-665.1
2000.0	-66.0
2160.0	151.0
2500.0	470.0
3000.0	880.0
3500.0	1260.0
4050.0	1711.7
4500.0	2165.1
4950.0	2707.7
5400.0	3415.3
5850.0	4379.2
6300.0	5698.5
6750.0	7462.8
7300.0	9717.4

POROSITY OF SOLID, From Source 3, Table 3.13-2

Degree of Char	Phi
0.000	0.01
1.000	0.345

WITH PLY PERMEABILITY, From Source 2, Reduced data, Table 3.2.1

Heating rate = 0.1 F/sec

Degree of Char	K, ft ²
0.00000	9.078E-17
0.00045	7.393E-17
0.00297	7.571E-17
0.01049	6.984E-17
0.02909	6.963E-17
0.06751	6.343E-17
0.13191	4.803E-17
0.21441	2.503E-17
0.72533	1.662E-14
0.82908	2.287E-14
0.89303	9.506E-14
0.93131	2.184E-13
0.99182	1.131E-12

ACROSS PLY PERMEABILITY, With ply permeability divided by 100

Degree of Char	K, ft ²
0.00000	9.078E-19
0.00045	7.393E-19
0.00297	7.571E-19
0.01049	6.984E-19
0.02909	6.963E-19
0.06751	6.343E-19
0.13191	4.803E-19
0.21441	2.503E-19
0.72533	1.662E-16
0.82908	2.287E-16
0.89303	9.506E-16
0.93131	2.184E-15
0.99182	1.131E-14

PYROLYSIS GAS MOLECULAR WEIGHT, From Source 4, Fig. 7

T, R	M, lbm/mole
1210.0	32.0
1460.0	26.0

PYROLYSIS GAS VISCOSITY, From Source 1, Sample 2

T, R	μ , lbf-s/ft ²
500.0	3.366E-7
720.0	4.127E-7
2880.0	9.988E-7
3600.0	1.151E-6
4320.0	1.299E-6
5040.0	1.450E-6
5760.0	1.618E-6
6500.0	1.713E-6